Virtual Network Mapping for Multicast Services With Max–Min Fairness of Reliability

Xiujiao Gao, Zilong Ye, Jingyuan Fan, Weida Zhong, Yangming Zhao, Xiaojun Cao, Hongfang Yu, and Chunming Qiao

***Abstract*—Network function virtualization (NFV) provides an effective way to reduce the network provider's cost by allowing multiple virtual networks (VNs) to share the underlying physical infrastructure. In the NFV environment, especially when supporting multicast services over the VNs, reliability is a critical requirement since the failure of one virtual node can cause the malfunction of multiple nodes that receive multicasting data from it. In this paper, we study for the first time to the best of our knowledge how to efficiently map VNs for multicast services over both general IP networks and orthogonal frequency division multiplexing (OFDM)-based elastic optical networks (EONs) while taking into consideration the max–min fairness in terms of reliability among distinct VNs. For general IP networks, we propose a mixed integer linear programming (MILP) model to determine the upper bound on the reliability with max–min fairness. In addition, an efficient heuristic, namely a reliability-aware genetic (RAG) algorithm, is developed to address reliable multicast VN mapping with a low computational complexity. By encoding multicast tree construction and link mapping into the process of path selection, taking into consideration the reliability with max–min fairness, and the networking reliability factors during mutation, RAG can globally optimize the reliability and fairness of all the multicast VN requests. For OFDM-based EONs, we extend the MILP (RAG) to optical-MILP [(O-MILP) optical RAG (O-RAG)] by considering the most efficient modulation format selection strategy, spectrum continuity, and conflict constraints. Through extensive simulations, we demonstrate that RAG (O-RAG) achieves close to the optimal reliability fairness with a much lower time complexity than the MILP (O-MILP) model. In particular, the path reliability-based mutation strategy in RAG (O-RAG) yields a significant performance improvement over other heuristic solutions in terms of reliability fairness, bandwidth (spectrum) consumption, and transmission delay.**

***Index Terms*—Elastic optical networks (EONs); Mixed integer linear programming (MILP); Multicast; Reliability with max–min fairness; Virtual network mapping.**

I. Introduction

Network function virtualization (NFV) provides an efficient and flexible way to deploy network services by implementing network functions in software that can run on standardized high volume servers/switches/storage. A set of network services can be provisioned through a virtual network (VN) (or service function chain [1,2]) consisting of virtual nodes and virtual links. The process of mapping a VN onto a substrate network (SN) generally includes two correlated processes: virtual node mapping and virtual link mapping. The former maps each virtual node onto a physical node that can provide sufficient computing/storage resources, while the latter maps each virtual link to a physical path with sufficient bandwidth/spectrum resources. With VN mapping in NFV, multiple diverse VNs can coexist on a common SN to share the physical resources, thus reducing the network provider's cost.

Many schemes have been proposed to address the general VN mapping problem for unicast services (e.g., [3–5]). Reliability has also been considered in such VN mapping [6–8] as a single physical node, or link failure may affect several VNs. However, there are few works focused on designing efficient strategies to accommodate multicast service-oriented VNs [9–12]. In fact, many big data applications, distributed file systems (e.g., Map-Reduce), point-to-multipoint real-time and interactive applications (e.g., video-conferencing and Internet protocol television) prefer multicast communications in order to improve the utilization of physical resources. Unlike the unicast service where data packets are transmitted between a single sender and a single receiver, multicast services require sending the same data to a selected group of destinations (or receivers), which can share the data transmission along the common links.

Recently, constructing reliable multicast tree routing directly in traditional fixed physical networks was investigated [13–17]. The authors of [13] minimized the routing cost in the multicast routing problem with delay and reliability constraint. The study in [14] introduced a reliable multicast routing algorithm based on a reliability test in multimedia communication that minimizes the network resource utilization for different reliability requirements of multicast requests. The authors of [15] investigated the problem of finding a k-hop multicast strategy with

Manuscript received June 17, 2015; revised July 26, 2015; accepted August 4, 2015; published August 28, 2015 (Doc. ID 242777).

Xiujiao Gao (e-mail: gaoxiujiao@gmail.com), Zilong Ye, Jingyuan Fan, Weida Zhong, Xiaojun Cao, and Chunming Qiao are with the Department of Computer Science and Engineering, SUNY-Buffalo, Buffalo, New York 14260, USA.

Yangming Zhao and Hongfang Yu are with the School of Communication and Information Engineering, University of Electronic Science and Technology of China, Chengdu, Sichuan 611731, China.

http://dx.doi.org/10.1364/JOCN.7.000942

1943-0620/15/090942-10$15.00/0

maximum reliability in directed tree networks and extended it into a general graph with an exponential time complexity. The work in [16] focused on developing high-throughput algorithms for reliable multicast routing in multihop wireless mesh networks. The work in [17] tried to find the one-to-many and many-to-many multicast trees with maximum reliability in a network with fixed topology.

In addition, orthogonal frequency division multiplexing (OFDM)-based elastic optical networks (EONs) that can efficiently select modulation formats and provide flexible spectrum allocation through assigning continuous finer grained subcarriers (i.e., 12.5 GHz) [18] are promising candidates for next generation optical networks of 100 Gbps, 400 Gbps, and beyond [19–21]. Provisioning multicast service over EONs has obtained attention because of its high bandwidth, low cost, and flexible spectrum allocation. For example, some solutions have been proposed to solve the multicast routing and spectrum allocation problem over EONs when source and destination nodes are given [22–25].

However, none of the above work considers how to efficiently map virtual networks for reliable multicast services while taking into consideration the max–min fairness in terms of reliability among distinct VNs. These works do not fully consider multicast routing together with virtual network mapping and multicast tree design so the proposed solutions cannot take advantage of the unique features of reliable multicast VN mapping. Specifically, reliable multicast VN mapping involves two types of sharing: data transmission sharing among multiple receivers within the same VN and SN sharing among multiple VNs. Hence, reliable unicast VN mapping and reliable multicast routing schemes in traditional fixed networks cannot be directly applied to efficiently mapping VNs for reliable multicast services. In addition, reliable multicast VN mapping has the following unique challenges: i) the physical multicasting source and destination nodes are not fixed; ii) the same multicasting streams over different virtual links may go through the same substrate link (e.g., fiber) to save bandwidth; iii) multicast VN mapping allows different multicast tree design (i.e., determining which destination nodes can be relay nodes to other destination nodes) to maximize network resource utilization; and iv) the mapping of source node and relay nodes needs to be more reliable since they may affect many other nodes.

As max–min fairness is an important quality of service (QoS) metric as shown in [26,27], we study in this paper the reliable multicast VN mapping problem with the objective of maximizing the reliability of the request that has the lowest reliability (the max–min fairness in terms of reliability) over general IP network and OFDM-based EONs.

We consider only the node reliability since link reliability issues can be straightforwardly converted into node reliability ones. For reliable multicast VN mapping over a general IP network, we propose a mixed integer linear programming (MILP) model to obtain the upper bound of the reliability with max–min fairness. We also design a reliability-aware genetic (RAG) algorithm with the following features: 1) RAG can jointly optimize node mapping, multicast tree construction, and link mapping by encoding them in one gene; 2) RAG converts multicast tree construction and link mapping into path selections to simplify the encoding process; 3) RAG combines the goal of max–min fairness in terms of reliability with the genetic evaluation objective so that it can obtain results close to the optimal solution; and 4) RAG adopts a path reliability-based mutation (PRM) mechanism, which can improve the mutation efficiency. For reliable multicast VN mapping over OFDM-based EONs, we formulate an optical-MILP (O-MILP) model by adding a modulation selection strategy, spectrum continuity, and conflict constraints to the MILP model for the general IP network scenario. O-MILP can obtain the upper bound of reliability with max–min fairness while considering modulation selection, spectrum continuity, and conflict constraints in OFDM-based EONs. We also propose an optical RAG (O-RAG) with additional features that can 1) achieve effective modulation selection by including the spectrum requirement in the gene encoding, and 2) satisfy spectrum continuity and nonconflict constraints with a first-fit strategy during the spectrum allocation process.

The remainder of this paper is organized as follows. We present the problem description, MILP model, and RAG algorithm for a general IP network in Section II. For OFDM-based EONs, we introduce the problem and present the proposed solutions, O-MILP and O-RAG, in Section III. The performance evaluation for both general IP networks and OFDM-based EONs is presented in Section IV. We conclude the paper in Section V.

II. Virtual Network Mapping for Reliable Multicast Services Over General IP Networks

A. Problem Description

A general substrate/physical network can be modeled as a graph $G_p = (V, E)$, where V is the set of physical nodes and E is the set of physical links. Each physical node v is equipped with $C(v)$ units of computation resources and a reliability constant $r_{pn}(v)$, while each link e has a bandwidth of $B(e)$.

For a given multicast VN request $MR_i = (s_i, D_i, b_i)$, $i \in R$, s_i is the virtual source node; D_i ($|D_i| > 1$) is the set of virtual destination nodes; and b_i is the requested bandwidth in the multicast group. We assume that a given node $v \in \{s_i, D_i\}$ requires $c(v)$ computing resources and can be mapped only onto a subset of physical nodes denoted by $S(v)$.

For each multicast request, we need to map the virtual nodes, construct a multicast tree (i.e., decide which nodes are "split and copy" nodes), and determine the routing such that the reliability of the mapped multicast request is maximized. For each MR_i, we normalize the expectation $E(D_i)$ of the number of live destination nodes in each multicast request as $E(D_i)/|D_i|$ to evaluate its reliability $R(MR_i)$. The primary reasons that we use $E(D_i)/|D_i|$ to measure the reliability of MR_i include the following: 1) for any multicast request, the scenario where only the source node survives is meaningless; 2) partial reliability (i.e., a subset of the destination nodes work) is acceptable in some multicast applications; and 3) the number of destination nodes are different among distinct multicast requests.

Given a multicast request MR_i and its tree topology mapping, the time to calculate $E(D_i)$ is exponential according to the definition of $E(D_i)$ as shown in

$$O(|V| * (C^1_{|D_i|} + C^2_{|D_i|} \cdots + C^{|D_i|}_{|D_i|})) = O(|V| * (2^{|D_i|} - C^0_{|D_i|})), \quad (1)$$

where $C^i_{|D_i|} = \frac{|D_i|!}{i! * (|D_i| - i)!}$.

To reduce the calculation complexity, we apply the linearity of expectation to obtain

$$E(D_i) = \sum_j E(d_{ij}) = \sum_j \prod_{v \in TN(d_{ij})} r_{pn}(v), \quad (2)$$

where $E(d_{ij})$ is the expectation of node $d_{ij} \in D_i$ that does not fail, and $TN(d_{ij})$ is the path from source node s_i to destination node d_{ij}. The time complexity of calculating $\sum_j E(d_{ij})$ in the worst case is $O(|V|)$.

Figure 1(a) shows an example of a multicast request MR_1 with three destination nodes. As shown in Fig. 1(b), s_1, d_{11}, d_{12}, and d_{13} can be mapped onto node B, F, C, and D, respectively. Node F is the mapping node for d_{11}, which is the split and copy node. The virtual link s_1–d_{11} is routed on link B–F; s_1–d_{12} is routed on links B–F–C; and s_1–d_{13} is routed on links B–F–D. The reliability $R(MR_1)$ of this mapping is $(E(d_{11}) + E(d_{12}) + E(d_{13}))/3$, where $E(d_{11}) = 0.9 * 0.9$, $E(d_{12}) = 0.9 * 0.9 * 0.8$, and $E(d_{13}) = 0.9 * 0.9 * 0.7$.

Since multiple multicast requests can share the same SN, it may not be fair to simply maximize the sum of the reliability of all the multicast requests when the SN resources are limited. In the following subsections, we propose solutions to maximize the reliability of the request that has the smallest reliability to achieve the max–min fairness among all the multicast requests.

B. Mixed Integer Linear Programming

In this subsection, we develop a MILP model to mathematically formulate the problem of multicast VN mapping with max–min fairness in terms of reliability over general IP networks. For each physical node, we pre-calculate K shortest paths to all the other nodes and the corresponding path reliabilities. The notations are listed in Table I.

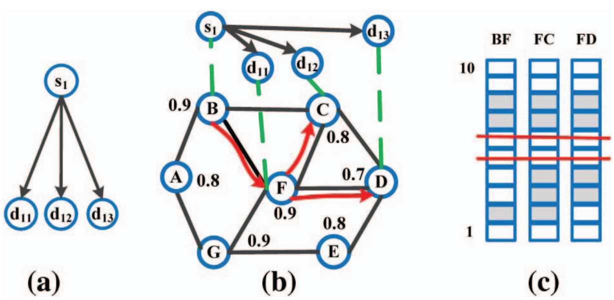

Fig. 1. Example of reliable multicast VN mapping.

Variables:

$$\sigma_{mn,i} = \begin{cases} 1, & \text{if } MR_i \text{ uses link } mn \in E_{AG} \\ 0, & \text{otherwise} \end{cases},$$

$$\eta_{k,ij} = \begin{cases} 1, & \text{if the traffic flow in } MR_i \text{ to node } d_{ij} \in D_i \\ & \text{goes through path } k \in |V| * (|V| - 1) * K \\ 0, & \text{otherwise} \end{cases}.$$

Objective:

The objective is to maximize the smallest reliability of all multicast requests mapping:

$$\text{Max} \min_{i \in R} R(MR_i), \quad (3)$$

$$R(MR_i) = \frac{\sum_j E(d_{ij})}{|D_i|} = \frac{\sum_{d_{ij} \in D_i} \sum_{k \in |V| * (|V|-1) * K} (r_p(k) * \eta_{k,ij})}{|D_i|}. \quad (4)$$

Constraints:

One-on-one node mapping:

$$\sum_{n \in S(s_i)} \sigma_{s_i n, i} = 1, \quad \forall\, i \in R, \quad (5)$$

TABLE I
NOTATIONS

Notation	Physical Meaning
$G_p = (V, E)$	A graph representing the physical SN
$v \in V$	A physical node
$C(v)$	The computing capacity of node v
$r_{pn}(v)$	The reliability of physical node v
$mn \in E$	The physical link between m and n
$B(mn)$	The bandwidth capacity of physical link mn
$\lvert V\rvert * (\lvert V\rvert - 1) * K$	The number of paths pre-calculated inside G_p
V^k	The set of nodes along the kth path
E^k	The set of links along the kth path
ps_k	The source node of the kth path
pd_k	The destination node of the kth path
$r_p(k)$	The path reliability of the kth path, which is the product of $r_{pn}(v)$, $\forall\, v \in V^k$
$MR_i = (s_i, D_i, b_i)$	A multicast request i
s_i	The source node of MR_i
$D_i(\lvert D_i\rvert > 1)$	The destination node set of MR_i
b_i	The requested bandwidth of MR_i
$V_i = \{s_i\} \cup D_i$	The node set for request MR_i
d_{ij}	The jth destination node in D_i
$c(v_i)$	The computation resource requirement of node $v_i \in V_i$
$S(v_i)$	The set of candidate physical mapping nodes of virtual node $v_i \in V_i$
E'	The set of links from the virtual source to its physical candidate mapping nodes and links from the destination's candidate physical mapping nodes to the corresponding destination
$E_{AG} = E \cup E'$	The augmented link set
$V_{AG} = V \cup (\cup_i V_i)$	The set of nodes from all requests and physical network
$G_{AG} = (V_{AG}, E_{AG})$	The augmented graph

$$\sum_{m\in S(d_{ij})} \sigma_{md_{ij},i} = 1, \quad \forall\, d_{ij}\in D_i, \quad \forall\, i\in R, \tag{6}$$

$$\sum_{m\in V_i} \sigma_{mn,i} \le 1, \quad \forall\, i\in R, \quad \forall\, n\in V. \tag{7}$$

Equations (5) and (6) ensure that each virtual node is mapped to one and only one physical node, and Eq. (7) ensures that multiple virtual nodes from the same request cannot be mapped to the same physical node.

Node capacity constraint:

$$\sum_{i\in R}\sigma_{s_i v,i} * c(s_i) + \sum_{i\in R}\sum_{d_{ij}\in D_i} \sigma_{vd_{ij},i} * c(d_{ij}) \le C(v), \ \forall v\in V. \tag{8}$$

Equation (8) specifies that the total computing resources allocated on any physical node $v\in V$ cannot exceed its capacity $C(v)$.

Link capacity constraint:

$$\sum_{i\in R}\sigma_{mn,i} * b(i) \le B(mn), \quad \forall\, mn\in E. \tag{9}$$

Equation (9) ensures that the total bandwidth allocated on any physical link $mn\in E$ cannot exceed its bandwidth capacity $B(mn)$.

Multicast tree construction:

$$\sum_{k\in|V|*(|V|-1)*K} \eta_{k,ij} = 1, \quad \forall\, j\in\{1,\ldots,|D_i|\}, \forall\, i\in R, \tag{10}$$

$$\sum_{j\in\{1,\ldots,|D_i|\}} \eta_{k,ij} \le 1, \quad \forall\, k\in |V| * (|V|-1) * K, \forall\, i\in R, \tag{11}$$

$$\sigma_{mn,i} = \begin{cases} 1, & \text{if } \eta_{k,ij} = 1, \forall\, i\in R, \forall\, j\in\{1,\ldots,|D_i|\}, \\ & \forall\, k\in K, \forall\, mn\in E^k \\ 0, & \text{otherwise} \end{cases}, \tag{12}$$

$$\sigma_{s_i ps_k,i} \ge \eta_{k,ij}, \quad \forall\, j\in\{1,\ldots,|D_i|\}, \quad \forall\, i\in R \tag{13}$$

$$\sigma_{pd_k d_{ij},i} \ge \eta_{k,ij}, \quad \forall\, j\in\{1,\ldots,|D_i|\}, \quad \forall\, i\in R. \tag{14}$$

Equation (10) shows that one and only one path will be selected for each source and destination pair in any multicast request. That the same path cannot be selected by more than one source destination pair for the same multicast request is represented in Eq. (11). In Eqs. (12)–(14), a link is marked as used by a multicast request i if the link belongs to any path that is used by multicast request i.

When K is large enough, the above linear programming model can obtain the optimal solution for the reliable multicast VN mapping problem. However, due to the computational complexity, the MILP model is infeasible for large-scale networks. Hence, in the next subsection, we propose a heuristic algorithm.

C. RAG Algorithm

In this subsection, we propose a RAG algorithm that jointly optimizes node mapping, multicast tree construction, and link mapping while considering physical network reliability during the mutation process to achieve max–min fairness in terms of reliability. In the following subsections, we present the encoding mechanism, fitness function, RAG design, and convergence condition for RAG.

1) Genetic Encoding and the Fitness Function: We encode each gene as the provisioning for a single multicast request. An individual composed of a set of different genes represents the provisioning for all multicast requests, and a population is a set of individuals. Specifically, we encode each Gene_i as $\{\{M(s_i, D_i)\}, \{R_{s_i d_{ij}}, d_{ij}\in D_i\}\}$ for a multicast request MR_i, where

- $\{M(s_i, D_i)\}$ represents the physical node mapping for virtual nodes (s_i, D_i);
- $\{R_{s_i d_{ij}}, d_{ij}\in D_i\}$ represents the physical routing path for virtual link (s_i, d_{ij}); and
- $R_{s_i d_{ij}}\in P_{s_i d_{ij}}$, $P_{s_i d_{ij}}$ is the set of physical path candidates for virtual link (s_i, d_{ij}) given node mapping in $\{M(s_i, D_i)\}$.

We calculate K, the most reliable paths (as defined in Table I) between each node pair (m, n) in the physical network, and denote them as PS_{mn}. When s_i is mapped onto physical node m and $d_{ij}\in D_i$ is mapped onto physical node n, we have $P_{s_i d_{ij}} = PS_{mn}$.

For each MR_i, we randomly select a node mapping $\{M(s_i, D_i)\}$, and then we randomly pick the routing paths $\{R_{s_i d_{ij}}, d_{ij}\in D_i\}$ for its multicast tree construction and link mapping. We apply this process for each multicast request to obtain an individual. Each request then can select a different node mapping and routing paths randomly (i.e., a new gene is created) to generate more individuals, and those different individuals are grouped together to form a population of size P.

To achieve reliability with max–min fairness, we set the fitness of each individual to be the lowest reliability among all the genes (i.e., mapping requests). The individual with a larger fitness value has a higher chance to survive in the evolution, thus RAG can obtain the max–min fairness in terms of reliability when it converges.

2) Design of RAG: The RAG procedure is shown in Algorithm 1. At the beginning of RAG, the first generation G of size P is initialized randomly, and then G goes into the evolution phase, which includes selection, crossover, and mutation operations. Specifically, a fixed number of individuals denoted as G_S are randomly selected from the population G; the tournament selection is applied within the individual set G_S (as shown in Step 2); and the winner of each tournament (i.e., the fittest one in the competing group) is selected to evolve to the crossover phase. In Step 3, we randomly pair all the winners as parents for multipoint gene level crossover to get offspring. For each parent pair, we randomly choose the $|R| * p_c$ (where p_c is the cross rate) number of genes to swap. We then select P fittest individuals from the parents' generation population and their offspring pools to keep the population size constant (as shown in Step 4). The chosen P fittest individuals then go into the mutation phase.

Algorithm 1 Reliability-Aware Genetic (RAG) Algorithm

1: Initialize the first generation G with population size P, and calculate the fitness value for each individual;
2: Select a subset G_S of G to participate in tournament selections;
3: Pair all the winners from tournament selection randomly for crossover to generate children;
4: Select P fittest individuals from parents and children, and then the chosen children go to the mutation phase;
5: For each chosen child, use PRM (Algorithm 2) to mutate the chosen genes;
6: Use the mutated child with an increased fitness value to replace the individual with the lowest fitness value until all the satisfied individuals are replaced while keeping the population size P constant to get new generation G';
7: If the RAG algorithm converges or reaches a preset threshold of an iteration number, go to **8**; otherwise go to **2** with G';
8: Provide reliable VN mapping according to the fittest individual in G', and terminate the process.

In the mutation phase, a number of genes are randomly selected by mutation ratio $|R| * p_m$ (where p_m is the mutation rate) for each offspring generated from the last crossover phase. For each chosen gene, we propose a PRM strategy as described in Algorithm 2 to generate a new mutated gene (as shown in Step 5 of RAG). The main idea of PRM is to select $\{M(s_i, D_i)\}$ for the chosen Gene$_i$ according to the uniform path reliability weight $W(v)$ of each physical node $v \in V$, and then randomly select $\{R_{s_i d_{ij}}, d_{ij} \in D_i\}$ to finish the mutation. $W(v)$ is not only the production of a uniform random value between (0, 1) but also the sum of the path reliabilities of all the candidate paths from node v to all the other nodes in physical node set V.

As shown in Steps 6–8 of Algorithm 1, the mutated child with the increased fitness value will replace the individual with the lowest fitness value to keep the population size unchanged. RAG then goes to the next evolution stage with this new generation. Once it converges, RAG will map all multicast requests according to the genetic encoding of the best fitness individual in the last generation.

Note that we adopt a self-adaptive strategy [28] to dynamically adjust the crossover rate p_c and mutation rate p_m based on the individuals' fitness as shown in Eqs. (15) and (16):

$$p_c = \begin{cases} \frac{F_{\max} - F'}{F_{\max} - F_{\text{mean}}}, & F' \geq F_{\text{mean}} \\ 1, & \text{otherwise} \end{cases}, \tag{15}$$

$$p_m = \begin{cases} \frac{F_{\max} - F_p}{F_{\max} - F_{\text{mean}}}, & F_p \geq F_{\text{mean}} \\ 0.5, & \text{otherwise} \end{cases}, \tag{16}$$

where F_p is the fitness of individual p; $F_{\max}$ is the largest fitness value in the population; F_{mean} is the average fitness value; and F' is the larger fitness value of two crossover individuals p_1 and p_2.

3) Convergence Condition: To evaluate RAG's convergence performance, we modify the degree of diversity [29] as in Eq. (17):

$$D_P = \frac{2}{P(P-1)} \sum_{p_1=1}^{P-1} \sum_{p_2=p_1+1}^{P} \frac{|D_F(p_1, p_2)|}{F_{\max}}, \tag{17}$$

where $|D_F(p_1, p_2)|$ is the absolute difference of the fitness of individual p_1 and p_2, and $F_{\max}$ is the maximum fitness value in the generation. If D_p is lower than a certain threshold for five or more generations [30], we say the algorithm has converged. We stop RAG when it converges or the number of iterations reaches a preset threshold.

III. Virtual Network Mapping for Reliable Multicast Services Over OFDM-Based EONs

A. Problem Description

Compared with virtual network mapping for reliable multicast service over general IP networks, mapping reliable multicast requests over OFDM-based EONs is more challenging because we need to consider efficient modulation selection and spectrum allocation with spectrum conflict and continuity constraints to establish optical channels during the link mapping. The detailed problem description is presented as follows.

An OFDM-based EON can be modeled as a graph $G_o = (V_o, E_o)$, where V_o is the set of physical nodes, and E_o is the set of fiber links. Each physical node v_o is equipped with $C(v_o)$ units of computation resources and a reliability constant $r_{pn}(v_o)$, while each fiber link can accommodate B subcarriers [the size of each subcarrier frequency slot (SFS) is 12.5 GHz]. The OFDM-based EONs use multicast-capable optical cross-connects (MC-OXCs), which can support four types of modulation formats: binary phase-shift keying (BPSK), quadrature phase-shift keying (QPSK), 8 quadrature amplitude modulation (QAM), and 16 QAM. The corresponding capacity of one SFS is $C^{\text{SFS}} = k * 12.5$ Gb/s, where $k = 1, 2, 3, 4$ with transmission reaches of 10,000, 5000, 2500, and 1250 km for the above four modulation formats, respectively. We assume that only BPSK can be used when the distance between the source and destination nodes is more than 10,000 km.

Algorithm 2 Path Reliability-Based Mutation (PRM)

1: For each physical node $v \in V$, generate a uniform random value between (0, 1) and update $W(v)$;
2: For the chosen Gene$_i$, select the physical node v' that has the largest $W(v')$ value from $S(s_i)$ as the mapping node for s_i, and add node v' into $\{M(s_i, D_i)\}$;
3: Select destination mapping nodes:
1) Find a physical node m in $V \backslash \{M(s_i, D_i)\}$ that has the largest $W(v)$ and mark it as the eligible candidate mapping node for some destination node $d_{ij} \in D_i$;
2) If there is more than one destination node using physical node $m \in V$ as the candidate mapping node, select node d_{ij}

with the least physical candidate mapping nodes to map first;
3) Map node d_{ij} onto physical node m; let $D_i = D_i \backslash d_{ij}$; and store node m in $\{M(s_i, D_i)\}$;
4: If $D_i \neq \Phi$, go to step **3**. Otherwise, randomly select $\{R_{s_i d_{ij}}, d_{ij} \in D_i\}$, and return to $\{\{M(s_i, D_i)\}, \{R_{s_i d_{ij}}, d_{ij} \in D_i\}\}$.

The multicast requests are the same as we described in Subsection II.A. For each multicast request, we need to find the one-on-one virtual node mapping, construct a multicast light-tree (i.e., decide which nodes are split and copy nodes in the optical domain), and determine the routing, modulation selection, and spectrum allocation of the light-tree over OFDM-based EONs such that the smallest reliability of the mapped multicast requests is maximized.

For example, if the substrate networks are the OFDM-based EONs in Fig. 1(b), we need to select modulation and allocate spectrum for the VN mapping. Assume the most efficient modulation format we can select under this mapping strategy is QPSK and the required spectrum slots of the multicast request are two subcarriers under the chosen modulation format. If the number of subcarriers on each fiber link is $B = 10$—as shown in Fig. 1(c), where the gray blocks represent the occupied subcarriers, and the blank ones are the available subcarriers—consecutive subcarriers 5 and 6 then can be selected to carry the multicast traffic on the mapped physical links B–F, F–C, and F–D. The reliability $R(MR_1)$ of this mapping is the same as the one calculated in Subsection II.A.

B. Optical Mixed Integer Linear Programming (O-MILP)

In this subsection, we develop a MILP model, namely O-MILP, to mathematically formulate multicast VN mapping with max–min fairness in terms of reliability over OFDM-based EONs. The objective is the same with the MILP we formulated in Subsection II.B. In addition to the notations, variables, and constraints in Table I, we list the notations, variables, and constraints that are unique to the OFDM-based EONs in this subsection.

Notations:

$d(mn)$: distance of fiber link $mn \in E_o$,
B: the number of subcarriers on each link in E_o,
B_{GB}: guard band between spectrum allocations for different requests.

Variables:

$$o_{ij} = \begin{cases} 1, & \text{if the starting spectrum slot for } MR_i \\ & \text{is smaller than that of } MR_i \\ 0, & \text{otherwise} \end{cases},$$

$$c_{ij} = \begin{cases} 1, & \text{if requests } MR_i \text{ and } MR_j \text{ use common link(s)} \\ 0, & \text{otherwise} \end{cases},$$

d_i: the maximal path length in the light-tree of MR_i,
n_i: the number of subcarriers that MR_i requires,
ss_i: an integer variable indicating the subcarrier allocation starting slot for request MR_i,
es_i an integer variable indicating the subcarrier allocation ending slot for request MR_i.

Constraints:

Modulation selection:

$$d_i = \max_{j \in \{1,\ldots,|D_i|\}} \sum_{mn \in E_o} \delta_{mn,ij} * d(mn), \quad \forall\, i \in R, \tag{18}$$

$$n_i = \lceil \frac{b_i}{C_i^{\mathrm{SFS}}} \rceil + B_{GB}. \tag{19}$$

Equation (18) calculates the distance of the longest path in the multicast light-tree. Equation (19) is used to calculate the number of subcarriers that MR_i requires, where C_i^{SFS} is determined by the reach distance d_i (when the most efficient modulation format is selected), as described in Subsection III.A.

Spectrum allocation constraint:

$$es_i - ss_i + 1 = n_i, \quad \forall\, i \in R, \tag{20}$$

$$es_i, ss_i \in (0, B], \quad \forall\, i \in R, \tag{21}$$

$$c_{ij} \geq \sigma_{mn,i} + \sigma_{mn,j} - 1, \quad \forall\, i,j \in R, i \neq j, \quad \forall\, mn \in E_o, \tag{22}$$

$$o_{ij} + o_{ji} = 1, \quad \forall\, i,j \in R, i \neq j, \tag{23}$$

$$es_j - ss_i + 1 \leq B(1 + o_{ij} - c_{ij}), \quad \forall\, i,j \in R, i \neq j, \tag{24}$$

$$es_i - ss_j + 1 \leq B(2 - o_{ij} - c_{ij}), \quad \forall\, i,j \in R, i \neq j. \tag{25}$$

Equation (20) shows that continuous subcarriers are allocated to the light-tree. Equation (21) is the spectrum capacity constraint. Equations (22)–(25) ensure that the spectrum conflict and continuity constraints are satisfied.

Since the O-MILP model is intractable for large-scale networks due to its time complexity, we extend our proposed RAG to solve the reliable multicast mapping over OFDM-based EONs in the next subsection.

C. Optical Reliability-Aware Genetic (O-RAG) Algorithm

In this subsection, we design an O-RAG algorithm. The main differences between O-RAG and the RAG in Section II are as follows: 1) O-RAG selects the most efficient modulation format through encoding each Gene$_i$ as $\{\{M(s_i, D_i)\}, \{R_{s_i d_{ij}}, d_{ij} \in D_i\}, n_i\}$, where n_i is the number of required spectrum slots using the most efficient modulation format for virtual node mapping $\{M(s_i, D_i)\}$ and virtual link mapping $\{R_{s_i d_{ij}}, d_{ij} \in D_i\}$. O-RAG calculates the longest virtual link routing path from $\{R_{s_i d_{ij}}, d_{ij} \in D_i\}$ and then applies Eq. (19) to calculate n_i, and 2) O-RAG uses

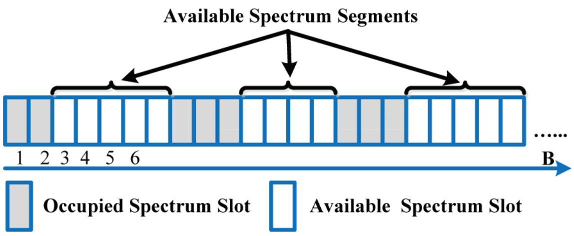

Fig. 2. Available spectrum segments.

the first-fit strategy to allocate n_i spectrum slots while following spectrum continuity and conflict constraints. More specifically, for each multicast request, all the links in the light-tree will use the same block of available spectrum segments as shown in Fig. 2.

IV. Performance Evaluation

A. Experimental Setting

We evaluate the proposed MILP/O-MILP model and heuristic algorithms on the 14-node and 22-link National Science Foundation Network (NSFNET). For a general IP network, each physical node can provide 10,000 units of computing resources, while each physical link in a general network has 4,000 units of bandwidth resources. Each physical node has a random reliability with a uniform distribution between 0.9 and 0.999. For OFDM-based EONs, the node features are the same as the general IP networks, but each fiber link has a spectrum capacity of 4.475 THz in the C band (i.e., 358 subcarriers), and the guard band for each request is one subcarrier [23].

For each multicast VN request, the number of destinations is uniformly distributed between 2 and 8. The computing demand of each node is less than 100 units with a uniform distribution. The set of candidate mapping nodes $S(v)$ (where $|S(v)|$ is within 3 and 14 following a uniform distribution) for each node v in the multicast request is randomly selected from the substrate node set. The bandwidth demand of each multicast request is uniformly distributed within 10–100 Gb/s.

The population size P is 50, and the tournament size is set to $0.35 * P$ (because $0.35 * P$ yields better performance in the simulation). The iteration number of RAG (O-RAG) is 1000, and $D_p = 1.0 \times 10^{-5}$.

We use IBM CPLEX to solve the MILP and Visual Studio to implement the heuristic algorithms. All simulations are run on a computer with a 2.5 GHz Intel Core i5-3210 CPU and 12 GB RAM. For the MILP, the simulation will be terminated if the optimal solution is obtained or the running time of 5 h is reached. We note that the largest optimality gap [according to the built-in function *GetMIPRelativeGap()* in CPLEX] in terms of reliability for all MILPs is 6.13×10^{-6}. Each statistical result is the average of 20 simulations.

To show the benefits of PRM (O-PRM), we implement another heuristic algorithm called No-PRM (O-No-PRM), which has the same steps as RAG (O-RAG) but uses a random mutation to replace the PRM in Step 5 of RAG (O-RAG). For comparison, we also implement a random mapping algorithm, namely Rand-Map (O-Rand-Map), which randomly maps nodes and links without considering reliability.

B. Performance Analysis

1) Performance Analysis Over General IP Networks: As shown in Fig. 3(a) [all the parts of Fig. 3 share the same legends as in Fig. 3(b)], we evaluate the reliability with max–min fairness of different solutions when the number of multicast requests increases. We can see that MILPK (K is the number of pre-calculated shortest paths between each physical node pair and $K = 1, 2, 3$) obtains higher reliability values as K increases because the larger K gives the MILP more path options for VN mapping. More specifically, MILP2 (MILP3) improves the reliability with max–min fairness by at most 0.4% (0.08%) compared to MILP1 (MILP2). We take the results from MILP3 as the approximate upper bound since the improvement ratio compared with MILP2 is small enough. We observed that the reliability with max–min fairness achieved by RAG is 0.2%–4% lower than the upper bound (which, however, may not be achievable when the number of requests is large) while increasing the reliability of No-PRM (Rand-Map) by 0.4%–3% (0.7%–4%). Such a reliability improvement percentage is significant when considering the yearly downtime of the system.

In Table II, we list the running time of different solutions when the number of multicast requests varies. We can see that RAG's running time is much smaller than that of

TABLE II
Running Time(s) of Different Solutions Over General IP Networks

	Number of Multicast Requests														
	3	5	8	10	12	15	20	25	30	40	50	60	80	100	120
MILP1	0.53	1.07	3.31	3.36	4.99	7.72	12.72	20.94	29.91	*	*	*	*	*	
MILP2	1.49	3.25	8.67	10.72	16.95	26.60	45.53	79.68	114.56	*	*	*	*	*	*
MILP3	3.07	6.67	19.16	23.82	36.85	60.10	104.41	186.23	268.20	*	*	*	*	*	*
RAG	0.19	0.37	0.69	0.79	1.09	1.21	1.58	2.21	2.52	3.11	3.75	4.33	5.97	7.53	9.42
No-PRM	0.17	0.37	0.50	0.77	1.06	1.28	1.53	1.81	1.96	2.61	3.07	4.01	4.45	5.69	6.49
Rand-Map	0.006	0.01	0.02	0.02	0.02	0.03	0.04	0.06	0.07	0.09	0.11	0.13	0.18	0.22	0.27

Note: * stands for an unreasonably long time.

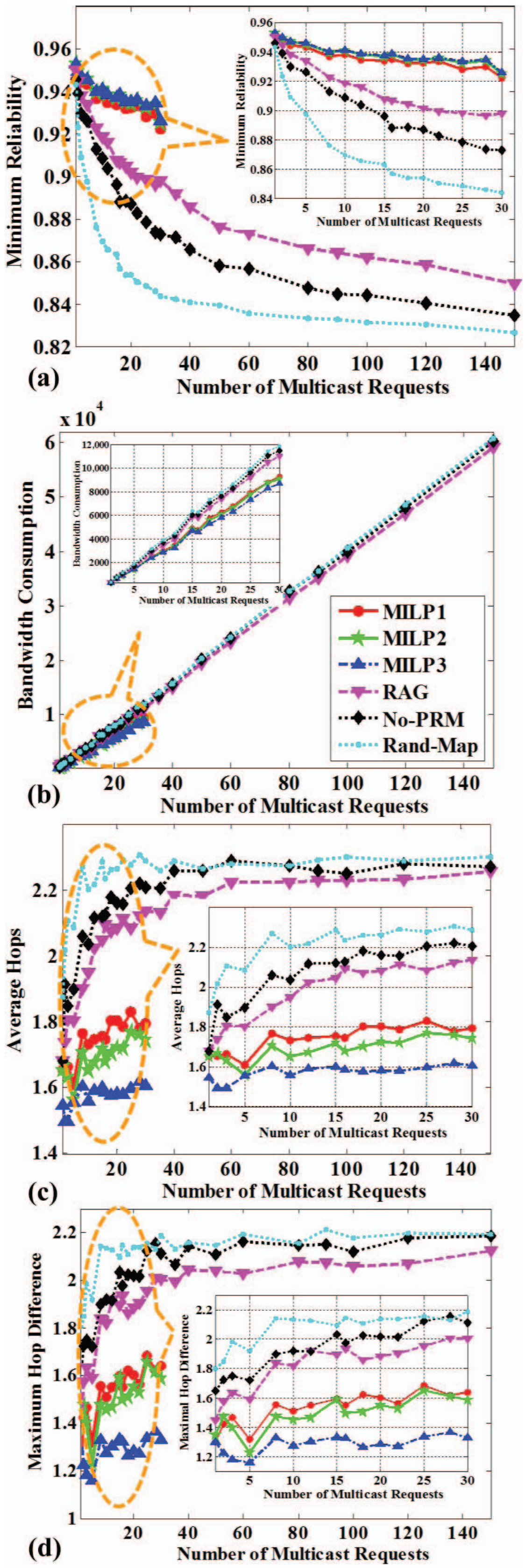

Fig. 3. Results of reliable VN mapping with max–min fairness over a general IP network.

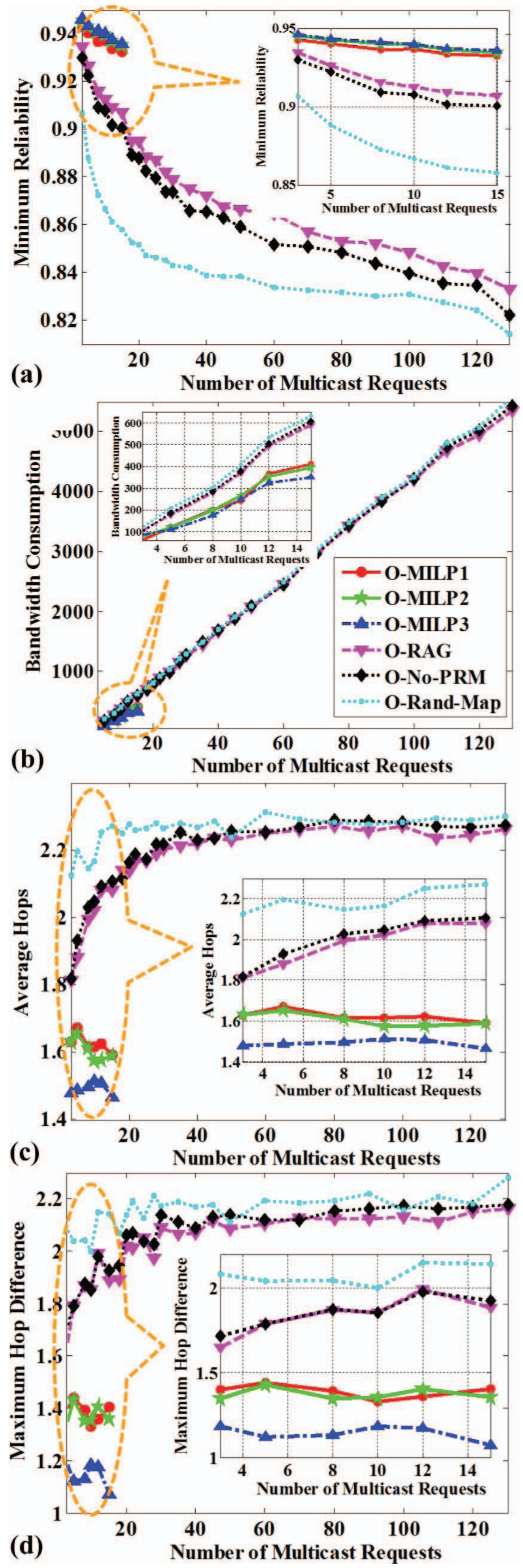

Fig. 4. Results of reliable VN mapping with max–min fairness over OFDM-based EONs.

TABLE III
RUNNING TIME(S) OF DIFFERENT SOLUTIONS OVER OFDM-BASED EONS

	Number of Multicast Requests														
	3	5	8	10	12	15	20	25	30	40	50	60	80	100	120
O-MILP1	0.82	2.08	4.56	8.67	11.74	28.04	*	*	*	*	*	*	*	*	*
O-MILP2	1.77	5.14	10.65	17.86	32.28	100.51	*	*	*	*	*	*	*	*	*
O-MILP3	3.28	9.51	20.75	37.60	75.92	244.04	*	*	*	*	*	*	*	*	*
O-RAG	0.62	1.04	1.72	2.19	2.47	3.24	4.34	5.08	6.43	7.19	9.43	13.92	14.19	17.98	19.85
O-No-PRM	0.49	0.93	1.44	2.09	2.77	3.24	4.55	5.24	5.87	7.02	8.51	9.58	12.84	12.36	14.21
O-Rand-Map	0.004	0.01	0.02	0.02	0.02	0.03	0.04	0.05	0.06	0.07	0.09	0.11	0.15	0.18	0.22

Note: * stands for an unreasonably long time.

MILP3 [which cannot find the optimal solution in a reasonable time (denoted by *) when the problem becomes large]. Hence, RAG can also be applied to the case with dynamic requests, particularly when the services are time-sensitive. Note that the actual provisioning time also depends on many other aspects of the network control plane, devices, subsystems, and so on and is out of the scope of this study.

We also evaluate the bandwidth consumption when the network resources are sufficient for a different number of multicast requests. From Fig. 3(b), we can observe that RAG requires 8% more bandwidth compared with MILP3, and consumes 5% and 10% less bandwidth compared with No-PRM and Rand-Map, respectively. The reason is that the more reliable a service is, the fewer hops it traverses, thus leading to a smaller amount of bandwidth consumption.

For delay-sensitive multicast service applications such as video-conferencing and distributed database replication, the transmission delay and the jitter among multiple destinations should be as small as possible. We use the average hops and the maximum hop difference among multiple destinations in the same multicast group to measure the delay bounds and jitter. From Figs. 3(c) and 3(d), we can observe that the average number of hops achieved by RAG is 5% (8%) smaller than that of No-PRM (Rand-Map) and the maximum hop difference is 6% (13%) smaller than that of No-PRM (Rand-Map), respectively. Hence, RAG is a computationally efficient solution that can achieve high reliability with max–min fairness while requiring less bandwidth resources, smaller transmission delay, and less jitter.

2) Performance Analysis Over OFDM-Based EONs: As shown in Fig. 4(a) [all the parts in Fig. 4 share the same legend as in Fig. 4(b)], we evaluate the reliability with max–min fairness of different solutions when the number of multicast requests increases in OFDM-based EONs. Similar to the case in general IP physical networks, we can see that O-MILPK (K is the number of pre-calculated shortest paths between each physical node pair and $K = 1, 2, 3$) obtains a higher reliability values as K increases. In fact, O-MILP2 (O-MILP3) improves the reliability with max–min fairness by at most 0.4% (0.08%) compared to O-MILP1 (O-MILP2). We observed that the reliability with max–min fairness achieved by O-RAG is close to the ones obtained by the O-MILP3 (1%–3% decrease ratio) while increasing the reliability of O-No-PRM (O-Rand-Map) by 0.4%–1% (2%–6%).

In Table III, we list the running times of different solutions when the number of multicast requests varies. We can see that O-RAG's running time is much shorter than that of the O-MILPs. The running time of O-MILPs (O-RAG) is larger than MILPs (RAG) because it needs to consider modulation selection and spectrum allocation during reliable multicast virtual network mapping.

We also evaluate the spectrum consumption when network resources are sufficient for different numbers of multicast requests. From Fig. 4(b), we can observe that O-RAG requires 40% more spectra compared with O-MILP3, and consumes 1% and 8% less bandwidth compared to O-No-PRM and O-Rand-Map, respectively. The reasons are two-fold. First, the more reliable a service is, the fewer hops it traverses. Second, the maximum distance of all links is smaller, thus more efficient modulation can be adopted to improve spectrum efficiency, which leads to a smaller amount of total spectrum consumption. From Figs. 4(c) and 4(d), we can observe that the average number of hops achieved by O-RAG is 1.5% (8%) smaller than that of O-No-PRM (O-Rand-Map), and the maximum hop difference is 1.5% (15%) smaller than that of O-No-PRM (O-Rand-Map), respectively. Hence, O-RAG is a computationally efficient solution that can achieve high reliability with max–min fairness and requires less spectrum resources, generates a smaller transmission delay, and produces less jitter than other heuristic solutions.

V. CONCLUSION

In this paper, we have investigated reliable multicast VN mapping over both general IP networks and OFDM-based EONs. For general IP networks, we have proposed a MILP model to maximize the reliability with max–min fairness. In addition, we have proposed the RAG algorithm that can jointly optimize the processes of virtual network mapping and multicast tree construction to obtain the max–min fairness in terms of reliability among multiple multicast virtual network requests. For OFDM-based EONs, we formulate another MILP model, the O-MILP, while considering the modulation selection and spectrum constraints to achieve high reliability with max–min fairness. We have also proposed the O-RAG algorithm, which embeds modulation selection in the process of gene encoding and considers spectrum continuity and conflict constraints in the process of spectrum allocation. Our simulation results have shown that the proposed RAG (O-RAG) can achieve outcomes that are close to the ones obtained by the MILP (O-MILP) and outperforms other heuristics in terms of reliability with max–min fairness, bandwidth (spectrum) consumption, and transmission delay.

There are several open problems related to reliable multicast VN mapping that deserve further study, including mapping multicasts with different reliability requirements while minimizing resource consumption, providing backups for multicast request mapping to achieve survivability, and reliable multicast VN mapping to tolerate large-scale co-related failures such as regional failures.

References

[1] "Network Function Virtualisation White Paper" [Online]. Available: http://portal.etsi.org/NFV/NFV_White_Paper.pdf.

[2] "Network functions virtualization-challenges and opportunities," Alcatel Lucent White Paper, 2013.

[3] Z. Cai, F. Liu, N. Xiao, Q. Liu, and Z. Wang, "Virtual infrastructure embedding for evolving networks," in *Proc. GLOBECOM*, 2010, pp. 1–5.

[4] M. Yu, Y. Yi, J. Rexford, and M. Chiang, "Rethinking virtual network embedding: Substrate support for path splitting and migration," *ACM SIGCOMM Comput. Commun. Rev.*, vol. 38, no. 2, pp. 17–29, 2008.

[5] N. M. M. K. Chowdhury, M. R. Rahman, and R. Boutaba, "Virtual infrastructure embedding with coordinated node and link mapping," in *Proc. IEEE INFOCOM*, 2009, pp. 783–791.

[6] O. Soualah, I. Fajjari, N. Aitsaadi, and A. Mellouk, "A reliable virtual network embedding algorithm based on game theory within cloud's backbone," in *Proc. IEEE Int. Conf. on Communications (ICC)*, June 2014, pp. 2975–2981.

[7] Q. Zhang, M. F. Zhani, M. Jabri, and R. Boutaba, "Venice: Reliable virtual data center embedding in clouds," in *Proc. IEEE INFOCOM*, 2014, pp. 289–297.

[8] W. Yeow, C. Westphal, and U. C. Kozat, "Designing and embedding reliable virtual infrastructures," *ACM SIGCOMM Comput. Commun. Rev.*, vol. 41, no. 2, pp. 57–64, Apr. 2011.

[9] M. Zhang, C. Wu, M. Jiang, and Q. Yang, "Mapping multicast service-oriented virtual infrastructures with delay and delay variation constraints," in *Proc. GLOBECOM*, 2010, pp. 1–5.

[10] X. Gao, Z. Ye, W. Zhong, C. Qiao, X. Cao, H. Zhao, H. Yu, and V. Anand, "Multicast service-oriented virtual network mapping over elastic optical networks," in *Proc. IEEE Int. Conf. on Communications (ICC)*, 2015, pp. 6796–6801.

[11] Y. Miao, Q. Yang, C. Wu, M. Jiang, and J. Chen, "Multicast virtual infrastructure mapping for supporting multiple description coding-based video applications," *Comput. Netw.*, vol. 57, no. 4, pp. 990–1002, Mar. 2013.

[12] P. Lv, Z. Cai, J. Xu, and M. Xu, "Multicast service-oriented virtual infrastructure embedding in wireless mesh networks," *IEEE Commun. Lett.*, vol. 16, no. 3, pp. 375–377, Mar. 2012.

[13] C. Yang and X. Zhao, "A multicast routing algorithm based on reliable transmission," in *Proc. IEEE IMSNA*, Dec. 2013, pp. 679–682.

[14] X. Qi, L. Liu, S. Liu, and J. Qiao, "A reliable multicast routing algorithm based on reliability test in multimedia communication," in *Proc. IEEE Int. Conf. on Communications, Circuits and Systems (ICCCAS)*, June 2004, vol. 1, pp. 596–600.

[15] M. I. Andreica and N. Tapus, "Maximum reliability *k*-hop multicast strategy in tree networks," in *Proc. IEEE ISCE*, Apr. 2008, pp. 1–4.

[16] X. Zhao, J. Guo, C. T. Chou, A. Misra, and S. K. Jha, "High-throughput reliable multicast in multi-hop wireless mesh networks," *IEEE Trans. Mob. Comput.*, vol. 14, no. 4, pp. 728–741, Apr. 2015.

[17] W. Ding, X. Wei, X. Nie, and M. Zhou, "Algorithms for finding maximum reliability many-to-many multicast routing under a fixed topology," in *Proc. IEEE ICNDC*, Oct. 2012, pp. 124–127.

[18] O. Gerstel, M. Jinno, A. Lord, and S. J. B. Yoo, "Elastic optical networking: A new dawn for the optical layer?" *IEEE Commun. Mag.*, vol. 50, no. 2, pp. S12–S20, Feb. 2012.

[19] P. Colbourne and B. Collings, "ROADM switching technologies," in *Proc. Optical Fiber Communication Conf. (OFC)*, Mar. 2011, pp. 1–3.

[20] A. Bocoi, M. Schuster, F. Rambach, M. Kiese, C.-A. Bunge, and B. Spinnler, "Reach-dependent capacity in optical networks enabled by OFDM," in *Proc. Optical Fiber Communication Conf. (OFC)*, Mar. 2009, pp. 1–3.

[21] H. Takara, T. Goh, K. Shibahara, K. Yonenaga, S. Kawai, and M. Jinno, "Experimental demonstration of 400 Gb/s multi-flow, multi-rate, multi-reach optical transmitter for efficient elastic spectral routing," in *Proc. IEEE European Conf. and Exhibition on Optical Communication (ECOC)*, Sept. 2011, pp. 1–3.

[22] X. Liu, L. Gong, and Z. Zhu, "On the spectrum-efficient overlay multicast in elastic optical networks built with multicast-incapable switches," *IEEE Commun. Lett.*, vol. 17, no. 9, pp. 1860–1863, Sept. 2013.

[23] L. Gong, X. Zhou, X. Liu, W. Zhao, W. Lu, and Z. Zhu, "Efficient resource allocation for all-optical multicasting over spectrum-sliced elastic optical networks," *J. Opt. Commun. Netw.*, vol. 5, no. 8, pp. 836–847, Aug. 2013.

[24] A. Patel, P. N. Ji, J. P. Jue, and T. Wang, "Light-tree establishment for optical multicasting in flexible optical WDM (FWDM) networks," in *Asia Communications and Photonics Conf. (ACP)*, Nov. 2012, pp. 1–3.

[25] Q. Wang and L. Chen, "Performance analysis of multicast traffic over spectrum elastic optical networks," in *Proc. Optical Fiber Communication Conf.*, 2012, pp. 1–3.

[26] Y. Li, Q. Peng, and X. Wang, "Multicast capacity with max-min fairness for heterogeneous networks," *IEEE/ACM Trans. Netw.*, vol. 22, no. 2, pp. 622–635, Apr. 2014.

[27] H. Lee, J. Cho, and S. Chong, "Distributed max–min flow control for multi-rate overlay multicast," *Comput. Netw.*, vol. 54, no. 11, pp. 1727–1738, Aug. 2010.

[28] M. Srinivas and L. M. Patnaik, "Adaptive probabilities of crossover and mutation in genetic algorithms," *IEEE Trans. Syst. Man Cybern.*, vol. 24, pp. 656–667, Apr. 1994.

[29] L. Gong, X. Zhou, W. Lu, and Z. Zhu, "A two-population based evolutionary approach for optimizing routing, modulation and spectrum assignments (RMSA) in O-OFDM networks," *IEEE Commun. Lett.*, vol. 16, no. 9, pp. 1520–1523, Sept. 2012.

[30] J. Koza, *Genetic Programming: On the Programming of Computers by Means of Natural Selection*. Cambridge, MA: MIT, 1992.